BIOLOGY OF REPRODUCTION **66,** 1259–1266 (2002)

Golgi Apparatus Dynamics During Mouse Oocyte In Vitro Maturation: Effect of the Membrane Trafficking Inhibitor Brefeldin A[1]

Ricardo D. Moreno,[4,6] Gerald Schatten,[3,7] and João Ramalho-Santos[2,4,5]

Center for Neuroscience and Cell Biology,[5] Department of Zoology, University of Coimbra, Coimbra, Portugal
Unit of Reproduction and Developmental Biology,[6] Department of Physiology, Pontifical Catholic University of Chile, Santiago, Chile
Division of Reproductive Sciences,[7] Oregon Regional Primate Research Center; Departments of Obstetrics and Gynecology, and Cell & Developmental Biology, Oregon Health & Science University, Portland, Oregon

ABSTRACT

We have studied Golgi apparatus dynamics during mouse oocyte in vitro maturation, employing both live imaging with the fluorescent lipid BODIPY-ceramide and immunocytochemistry using several specific markers (β-COP, giantin, and TGN38). In germinal vesicle oocytes the Golgi consisted of a series of structures, possibly cisternal stacks, dispersed in the ooplasm, but slightly more concentrated in the interior than at the cortex. A similar pattern was detected in rhesus monkey germinal vesicle oocytes. These "mini-Golgis" were functionally active because they were reversibly disrupted by the membrane trafficking inhibitor brefeldin A. However, the drug had no visible effect if the oocytes had been previously microinjected with GTP-γ-S. During in vitro maturation the large Golgi apparatus structures fragmented at germinal vesicle breakdown, and dispersed homogenously throughout the ooplasm, remaining in a fragmented state in metaphase-II oocytes. Similarly to what has been reported using protein synthesis inhibitors, the presence of brefeldin A blocked maturation at the germinal vesicle breakdown stage before the assembly of the metaphase-I spindle. These results suggest that progression of murine oocyte maturation may require functional membrane trafficking.

gamete biology, gametogenesis, meiosis, oocyte development

INTRODUCTION

In sexually mature mice, fully grown oocytes resume meiosis and complete the first meiotic reductive division just before ovulation. Resumption of meiosis can be mediated in vivo by a hormonal stimulus or it can take place in vitro simply by oocytes being released from their ovarian follicle into a suitable medium. Meiotic maturation is characterized by dissolution of the nuclear membrane of the oocyte germinal vesicle (GV) (a process known as germinal vesicle breakdown; GVBD), condensation of chromatin into bivalents, chromosome alignment in the metaphase I spindle (MET I), and separation of homologous chromosomes. These events are followed by emission of the first polar body and arrest of meiosis with the chromosomes aligned at the metaphase II spindle. Protein synthesis varies throughout this period [1], and protein synthesis inhibitors block spontaneous mouse oocyte in vitro maturation (IVM), although inhibition takes place only at the GVBD stage [2–5]. This block is characteristic of rodent oocytes because oocytes from domestic species (cows, pigs, and sheep) require the production of novel proteins to initiate maturation, and progress beyond the GV stage [6–9]. At the molecular level, meiotic maturation is controlled through the activation of M-phase promoting factor (MPF), which is regulated, in turn, by the synthesis and degradation of its regulatory subunit, cyclin B [10–13]. In mouse occytes, cyclin B reaches its maximum level at the end of the first M phase, it is degraded at the time of first polar body extrusion, and is synthesized again to prepare the oocyte for the second meiotic division [11, 12]. Inhibition of protein synthesis blocks rodent oocyte IVM at the GVBD stage because a pool of preexisting cyclin B is available to reinitiate meiosis; however, the inability to synthesize new cyclin B prevents the oocyte from progressing further [12–14].

Although much is known about the molecular switches required for the triggering of IVM, membrane trafficking, which is an important feature of eukaryotic cells, involving intraorganelle shuttling of material packaged in transport vesicles, has received little attention in oocyte maturation studies. However, some information is available on organelle dynamics, particularly at the structural level [15–20]. Once oocyte growth has begun, a single Golgi apparatus is no longer visible, but many Golgi stacks appear in the ooplasm [15, 16]. These stacks are then fragmented, and remain in that form in oocytes arrested at metaphase II [15, 21, 22]. It is also well known that the Golgi apparatus undergoes extensive fragmentation when somatic cells enter mitosis [23–25]. This fragmentation can be mimicked by incubating the cells with a microtubule-disrupting drug such as nocodazole [26]; nonetheless, whether these two phenomena are equivalent is still under debate.

In this work we have focused our attention on the Golgi apparatus of mouse GV oocytes, as well as on the dynamics of this organelle during murine oocyte IVM. The Golgi apparatus plays a central role in many intracellular trafficking events; both related to protein synthesis and delivery and to processing of molecules internalized via the endocytic pathway [27–32]. To probe Golgi activity we have relied on both vital labeling and immunofluorescence, and

[1]This work was supported by research grants from the National Institute of Child Health and Human Development, and the National Center for Research Resources to G.S. J.R.-S. was the recipient of a Praxis XXI postdoctoral fellowship from Fundação para a Ciência e Tecnologia of Portugal.
[2]Correspondence: João Ramalho-Santos, Department of Zoology, University of Coimbra, Largo Marquês de Pombal, 3004-517 Coimbra, Portugal. FAX: 351 239 826798; e-mail: jramalho@ci.uc.pt
[3]Current address: Pittsburgh Development Center, Magee-Women's Research Institute, University of Pittsburgh, 204 Craft Avenue, Pittsburgh, PA 15213.
[4]R.D.M. and J.R.-S. contributed equally to this work.

Received: 2 August 2001.
First decision: 27 August 2001.
Accepted: 27 November 2001.

ISSN: 0006-3363. http://www.biolreprod.org

we have employed the fungal metabolite brefeldin A, a drug that inhibits protein secretion by blocking membrane trafficking from the endoplasmic reticulum (ER) to the Golgi apparatus [33]. Specifically, brefeldin A inhibits the formation of a specific type of vesicular carrier that participates in anterograde/retrograde membrane transport in the ER and Golgi. These vesicles are coated with a nonclathrin coatomer, which is formed from several subunits of coat proteins, and are thus known as COPI-vesicles [28, 33, 34]. As a result, the well-defined Golgi apparatus is dispersed throughout the cytoplasm, possibly being redistributed to the ER, both in somatic and spermatogenic cells [28, 33, 35, 36]. Brefeldin A sensitivity can thus be used to assess the state of the Golgi apparatus as well as ER-Golgi vesicular transport in a given cell.

MATERIALS AND METHODS

Chemicals and Antibodies

All chemicals were obtained from Sigma Chemical Company (St. Louis, MO) unless otherwise stated. Rabbit polyclonal antibodies against Giantin were a kind gift from Dr. Edward K.L. Chan of The Scripps Institute, La Jolla, CA. Antibodies against TGN38 and β-COP were from Affinity Bioreagents Inc. (Golden, CO). The monoclonal antibody mAb414 (BabCo, Berkeley, CA) was used to detect nuclear pore complexes [37].

Isolation of Mouse GV Oocytes and IVM

Female ICR mice were stimulated i.p. with 5 IU of eCG 48 h before their ovaries were collected. Denuded GV-stage oocytes were obtained by dissecting the ovaries into warm M2 culture medium [38] supplemented with 100 μg/ml dibutyrylcyclic AMP (dbcAMP) to prevent GVBD, as described [2, 20, 39]. Cumulus cells were removed mechanically, and only intact, well-defined GV oocytes were used. The oocytes were distributed in groups of about 10, placed in medium droplets under mineral oil, and cultured at 37°C in an incubator. Media composition and incubation times varied with the experimental purpose (see *Results*). An energy-depleted version of the M2 culture medium was also developed. For this purpose, glucose was substituted with deoxyglucose, sodium azide was added (0.05% w/v), and sodium pyruvate and sodium lactate were removed from the medium. To maintain osmolarity, NaCl and KCl concentrations were increased so that the NaCl:KCl ratio of 20:1, which was present in the original medium, was retained. For IVM experiments the oocytes were washed out of dbcAMP, placed in droplets of fresh M2 medium, and incubated overnight. Oocytes were checked for GVBD 1–3 h after the triggering of IVM [2, 39]. Completion of IVM was assessed the following morning by first polar body extrusion (metaphase II or first polar body oocytes). IVM was also confirmed by immunocytochemistry. The features monitored included the formation of a metaphase II spindle, and the presence of a cortical granule-free area surrounding the spindle. For control purposes, IVM first polar body oocytes were activated with 5% ethanol, and activation was assessed by second polar body extrusion, pronuclear formation, and changes in cortical granules.

Isolation of Rhesus Monkey GV Oocytes

Rhesus macaque (*Macaca mullata*) GV oocytes were obtained from females exhibiting normal menstrual cycles, and which had been hyperstimulated by a regimen of exogenous gonadotropic hormones, as described in detail elsewhere [40]. Oocytes were collected by follicular aspiration using laparoscopy, and GV oocytes were selected and processed for immunocytochemistry (see below).

Live Imaging of Golgi Apparatus

The zona pellucida of mouse GV oocytes was removed by a short incubation in acid Tyrode medium, and the naked oocytes were placed in dbcAMP-supplemented M2 medium containing 5 μM of the fluorescent lipid BODIPY FL-C5-ceramide (Molecular Probes, Eugene, OR) and incubated in the dark for 2 h [35, 36, 41]. The oocytes were then washed in fresh dbcAMP-supplemented M2, incubated for an additional 0.5–1 h, and visualized by epifluorescence microscopy using a Zeiss Axiophot (Carl Zeiss, Thornwood, NY) or a Nikon Eclipse E1000 (Nikon, Melville, NY) epifluorescence-equipped microscope operated with Metamorph software (Universal Imaging, West Chester, PA).

Microinjection of Mouse GV Oocytes

Immature mouse oocytes at the GV stage were obtained as described above. Fully grown oocytes were maintained in dbcAMP-containing M2 medium. Immature oocyte volume was calculated, and a maximum of 5% of the egg volume was injected. Micropipettes were calibrated and front-loaded with a solution of GTP-γ-S prepared in M2 medium. Calculating the dilution inside the oocyte, the final concentration of GTP-γ-S in the ooplasm was estimated to be 40 mM. In order to make sure the microinjection procedure was successful, GTP-γ-S was coinjected with Texas Red-labeled BSA (Molecular Probes). In addition, for control purposes, one group of oocytes was injected with Texas Red-BSA alone. The survival rate of injected oocytes was 50%–60%, both for experimental and control (injection of Texas Red-BSA alone) groups, and only intact oocytes were used for experiments. Following GTP-γ-S microinjection, the oocytes were returned to dbcAMP-containing M2 medium, exposed to brefeldin A, and processed for immunocytochemistry as described below.

Brefeldin A Treatment

Oocytes arrested at the GV stage were placed in dbcAMP-containing M2 medium with varying concentrations (see *Results*) of the fungal metabolite brefeldin A (Epicentre Technologies, Madison WI) and incubated at 37°C for 20 min to 1 h. In some cases oocytes were fixed following brefeldin A treatment and processed for immunocytochemistry as described below. In other experiments the drug was washed out, and the oocytes were placed in fresh dbcAMP-containing M2, and further incubated for 1 h at 37°C. In vitro maturation experiments were also performed in the presence of varying concentrations of brefeldin A (see *Results*). Statistical analysis was carried out using the Student-Newman-Keuls, or the Tukey-Kramer, multiple comparisons tests.

Immunocytochemistry

For immunocytochemistry the zona pellucida of mouse and rhesus oocytes was removed by a short incubation in acid Tyrode medium, and the oocytes were gently attached to poly-L-lysine-coated coverslips in calcium-free medium. Fixation was carried out by adding 2% formaldehyde, followed by a 1- to 2-h incubation. The samples were then permeabilized for 60 min in PBS containing 1% Triton X-100, and nonspecific reactions were blocked by further incubation in PBS containing 2 mg/ml BSA and 100 mM glycine. For labeling, the antibodies were solubilized in this blocking solution and incubated with the coverslips for 1–2 h at the appropriate dilutions. After extensive washing in PBS containing 0.1% Triton X-100, the samples were sequentially labeled with either TRITC-conjugated or fluorescein isothiocyanate (FITC)-conjugated (Zymed, San Francisco, CA), or Alexa-488 or Alexa-568 (Molecular Probes) appropriate secondary antibodies for 1 h, and the DNA stain 4′-6′-diamino-2-phenylindole (DAPI; Molecular Probes) for 5 min. For cortical granule labeling oocytes were incubated for 1 h with a 10-μg/ml solution of FITC-tagged *Lens culinaris* agglutinin (LCA-FITC; EY Laboratories, San Mateo, CA), as reported previously [42]. Following these incubations, coverslips were mounted in VectaShield mounting medium (Vector Laboratories, Burlingame, CA) and sealed with nail polish. Samples were examined with a Zeiss Axiophot or a Nikon Eclipse E1000 epifluorescence-equipped microscope operated with Metamorph software. Confocal imaging was carried out with a Leica TCS NT confocal microscope (Leica Microsystems, Bannockburn, IL).

RESULTS

Imaging the Golgi Apparatus in Mouse GV Oocytes

Using the fluorescent Golgi-specific lipid BODIPY-ceramide we were able to visualize the Golgi apparatus in live GV oocytes, arrested in dbcAMP-containing M2 medium (Fig. 1). Laser scanning microscopy of GV oocytes labeled with BODIPY-ceramide revealed a number of independent structures that were either sausage-shaped or amorphous. The labeling was reminiscent of the dispersion of Golgi fragments throughout the cytoplasm that takes place in somatic cells following nocodazole treatment [26]. These stacks, or ''mini-Golgis,'' were more concentrated in the

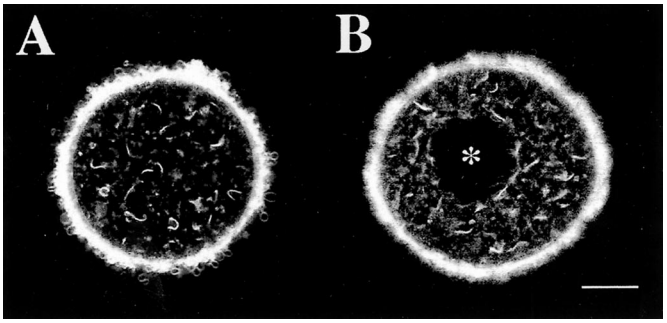

FIG. 1. Live imaging of Golgi apparatus in mouse GV oocytes using BODIPY-ceramide. Golgi apparatus of GV-arrested oocytes was labeled with fluorescence-tagged ceramide and imaged using laser scanning confocal microscopy. Both cortical (**A**) and internal (**B**) focal planes are shown. *Position of the germinal vesicle. Bar = 20 μm.

interior of the oocyte (Fig. 1B), although they were also present at the cortex (Fig. 1A). Staining on the oocyte surface, observed as a halo, is the likely result of probe attachment to remnants of the zona pellucida.

The nature of these mini-Golgis in mouse GV oocytes was confirmed by immunocytochemistry using the well-known Golgi marker β-COP, a protein that is also present in COPI vesicle coats. In dbcAMP-arrested GV oocytes the β-COP probe stained a large number of aggregates (Fig. 2A), similar to the structures labeled by BODIPY-ceramide, and these structures were also less abundant closer to the cortex (not shown). At this stage most cortical granules, as detected by LCA-FITC staining, were found close to the oocyte surface (Fig. 2B), with only a few present in the interior (not shown). Maintenance of a β-COP staining pattern in a dynamic Golgi apparatus is energy-dependent. Indeed, if GV oocytes were placed for 20–30 min in an energy-depleted version of the M2 medium (see *Materials and Methods*) containing dbcAMP, no distinct structures were labeled by the Golgi marker (Fig. 2A′), although the cortical granule distribution (Fig. 2B′) and DNA (not shown) remained unchanged. Furthermore, this distribution of mini-Golgi stacks in the ooplasm of GV-arrested oocytes was not exclusive to the mouse, because similar structures could be detected in rhesus monkey GV oocytes (Fig. 3), using both β-COP (Fig. 3A) and giantin (Fig. 3B) as markers for the organelle, suggesting a general pattern common to mammalian oocytes.

Brefeldin A Disrupts the Golgi Apparatus in Mouse GV Oocytes

To determine whether the Golgi apparatus is functionally active in GV-arrested mouse oocytes we incubated the oocytes in M2 medium containing both dbcAMP and brefeldin A (5–10 μM). This treatment resulted in visible and reversible redistribution of β-COP into the ooplasm (data not shown). However, it has been shown that brefeldin A can induce the release of β-COP from the Golgi apparatus into the cytoplasm of somatic cells without affecting redistribution of the organelle to the endoplasmic reticulum. Therefore, we decided to evaluate the integrity of the Golgi apparatus using the transmembrane *cis*-Golgi marker giantin, a protein that is present in both Golgi stacks and COPI vesicle coats (Fig. 4, A–D). Whereas control GV oocytes showed the same mini-Golgi pattern described above (Fig. 4A), the ooplasm of brefeldin A-treated oocytes had no distinct structures, as evaluated using the antigiantin probe (Fig. 4B). Given that in somatic cells the effect of brefeldin

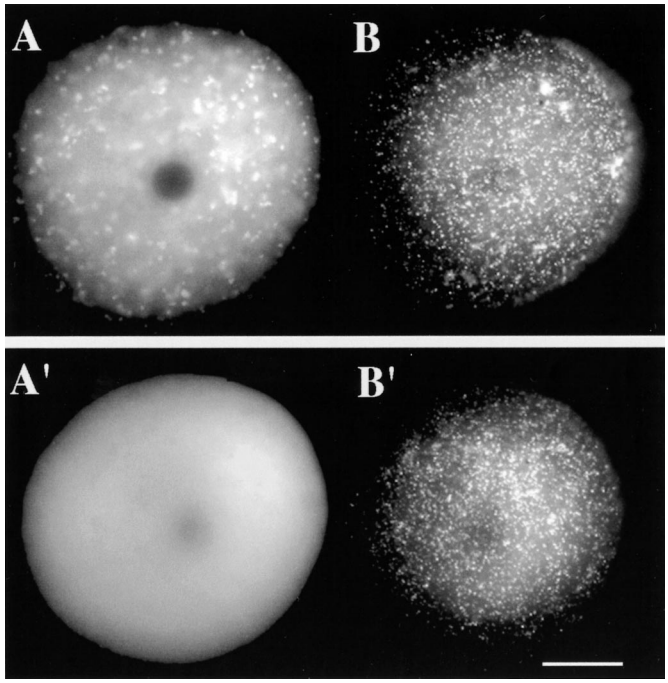

FIG. 2. Golgi apparatus in mouse GV oocytes as visualized using β-COP. Effect of energy deprivation. Golgi apparatus of GV-arrested oocytes was labeled by immunocytochemistry using the β-COP antibody, in both control oocytes (**A**) and oocytes placed in an energy-depleted medium (**B**). A focal plane through the center of the oocyte is shown in each case. The cortical distribution of cortical granules, observed with LCA-FITC, is also shown for **A** and **B** (**A′** and **B′**, respectively). Bar = 20 μm.

A is reversible, we washed out the drug and allowed the oocytes a 1-h recovery period in fresh dbcAMP-containing M2 medium. Following recovery the Golgi aggregates were again visible in the ooplasm, and were similar to those seen in control samples (Fig. 4C). However, the disruptive effect of brefeldin A on Golgi structure was prevented in oocytes that had been previously injected with GTP-γ-S, a nonhydrolyzable GTP analogue (Fig. 4D, compare with Fig. 4B). In addition, incubation of GV oocytes with brefeldin A had no effect on the surface pattern of cortical granules, as visualized using LCA-FITC (Fig. 4, E and F).

To confirm these observations of the effect of brefeldin A on the Golgi apparatus we repeated the experiment using confocal microscopy and a marker for the trans-Golgi network, the integral membrane protein TGN38 (Fig. 5). In control GV oocytes, large TGN38-positive structures were visible, similar to the patterns detected with ceramide, β-COP, and giantin (Fig. 5A). In this case it was possible to determine that the large Golgi aggregates seemed to be 1–

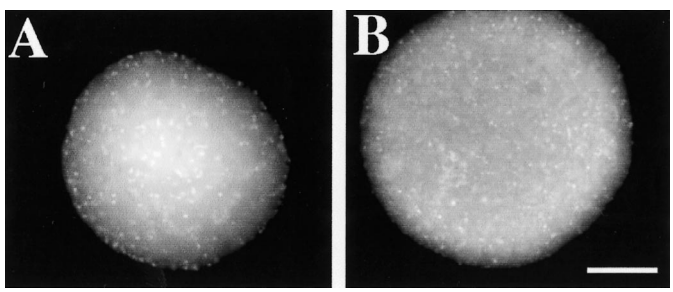

FIG. 3. Golgi apparatus in rhesus monkey GV oocytes was imaged by immunocytochemistry using both β-COP antibody (**A**) and an antigiantin probe (**B**). Bar = 20 μm.

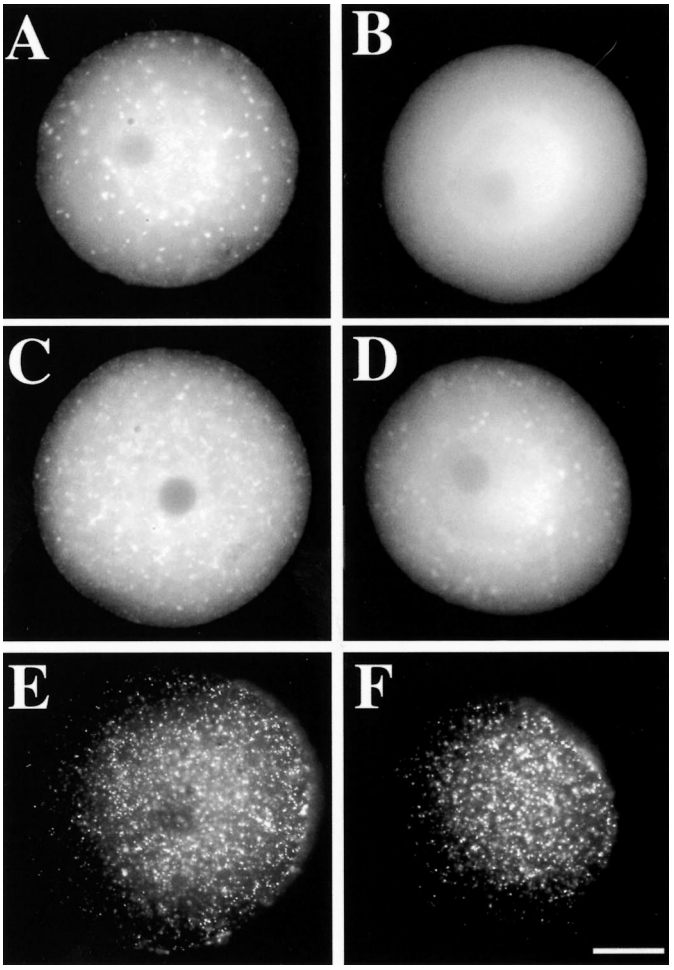

FIG. 4. Effect of brefeldin A on the Golgi apparatus and cortical granules of mouse GV oocytes. The Golgi apparatus was imaged by immunocytochemistry using an antigiantin probe, both before (**A**), and after, a 1-h incubation in M2 medium containing both dbcAMP and 5 μM brefeldin A (**B**). Following this incubation the drug was washed out and oocytes were visualized after a 1- to 2-h recovery period in dbcAMP containing M2 (**C**). The effect of brefeldin A was also evaluated in GV oocytes that had previously been injected with a final ooplasmic concentration of 40 mM GTP-γ-S (**D**). An equivalent focal plane through the center of the oocyte is shown in each case. The effect of brefeldin A on the cortical granule pattern at the surface of GV oocytes was also monitored using LCA-FITC. **E**) Control oocyte kept in dbcAMP-containing M2 medium. **F**) Oocyte imaged following a 1-h incubation in M2 medium containing both dbcAMP and 5 μM brefeldin A. Bar = 20 μm.

3 μm long (Fig. 5A′). Following brefeldin A treatment these aggregates were no longer visible, and a punctated pattern emerged, similar to that observed with giantin (Fig. 5, B and B′). When the oocytes were allowed to recover in M2 medium lacking the fungal metabolite, larger Golgi structures were again visible in the ooplasm (Fig. 5C), although confocal microscopy allowed us to determine that they were smaller than those present in control GV oocytes (Fig. 5C′). However, we were able to establish that these recovered oocytes progressed normally through IVM, and were able to extrude the first polar body if placed in M2 medium lacking dbcAMP. First polar body extrusion took place in 68.3% ± 4.0 SEM of control oocytes, and in 73.0% ± 6.2 SEM recovered oocytes ($P > 0.05$); by comparison, oocytes maintained in brefeldin A showed only a 2.7% ± 2.1 SEM rate of first polar body extrusion ($P < 0.001$, relative to the other two groups). Subsequently, these matured (recovered) oocytes could be parthogenetically activated in the presence of 5% ethanol, similar to control oocytes. Control oocytes showed a 65% ± 7.8 SEM activation rate, whereas in recovered oocytes that rate was 68% ± 5.5 SEM ($P > 0.05$). Taken together these results suggest that the effect of brefeldin A on mouse GV oocytes is indeed fully reversible.

Brefeldin A Inhibits Mouse Oocyte IVM

Disruption of the Golgi apparatus in GV-arrested mouse oocyte following brefeldin A treatment was reminiscent of what takes place during normal IVM, triggered by placing the oocytes in dbcAMP-free M2 medium (Fig. 6). In GV oocytes, Golgi structures, as visualized using the giantin antibody, are conspicuous in the ooplasm, which also features a well-defined nucleopore-containing nuclear envelope (Fig. 6A). At GVBD the nuclear envelope is dismantled, the chromosomes condense, and the mini-Golgis dissolve, showing an accumulation of dotted structures in the central part of the oocyte (Fig. 6B). The Golgi fragments spread more evenly throughout the oocyte in metaphase-I (Fig. 6C), and this distribution is maintained following extrusion of the first polar body in metaphase-II (Fig. 6D) oocytes. It is curious that a slight accumulation of giantin-positive structures was often detected at the spindle poles in this case (Fig. 6D), similar to what has been described for the mitotic spindle of somatic cells.

It is interesting that brefeldin A arrested mouse oocyte IVM after the onset of GVBD, the stage during which Golgi fragmentation takes place (Fig. 7). Although some apparently healthy oocytes arrest at different stages of maturation, even in control samples, the effect of brefeldin A was evident, virtually abolishing the conclusion of IVM, as assessed by first polar body extrusion. The concentration dependency of this drug effect was quite abrupt. No statistically significant changes were detected within a 0.5–50 nM range of concentrations, compared with control samples obtained on the same day (Fig. 7). However, the effect was maximal at 0.5 μM brefeldin A, and higher concentrations had no further effect (Fig. 7). Imaging the DNA by fluorescence microscopy showed no distinct metaphase I arrangements in brefeldin A-arrested oocytes, although the chromosomes were condensed (data not shown). The reversibility of this inhibition was dependent on the time of incubation. Thus, when oocytes were incubated in M2 with 0.5 μM brefeldin A for up to 6 h they could still complete first polar body extrusion, provided the drug was washed out, and the incubation continued in brefeldin A-free M2 medium. The rate of first polar body extrusion in these recovered oocyes was 69.7% ± 4.5 SEM, comparable to the 71.9 ± 2.3 SEM rate found in control occytes ($P > 0.05$).

DISCUSSION

The Golgi apparatus in mouse GV oocytes is well developed, and consists of a series of aggregates that can be visualized dynamically using BODIPY-ceramide, and by immunocytochemistry. These large structures likely correspond to the series of Golgi stacks (or dictyosomes) described in many previous works in mouse and hamster oocytes using ultrastructural analysis by electron microscopy [15, 16, 21, 22].

The Golgi stacks of both mouse and rhesus GV oocytes clearly resemble the mini-Golgis described in somatic cells after microtubule disruption induced by nocodazole treatment [26]. It should be noted that, besides a microtubular

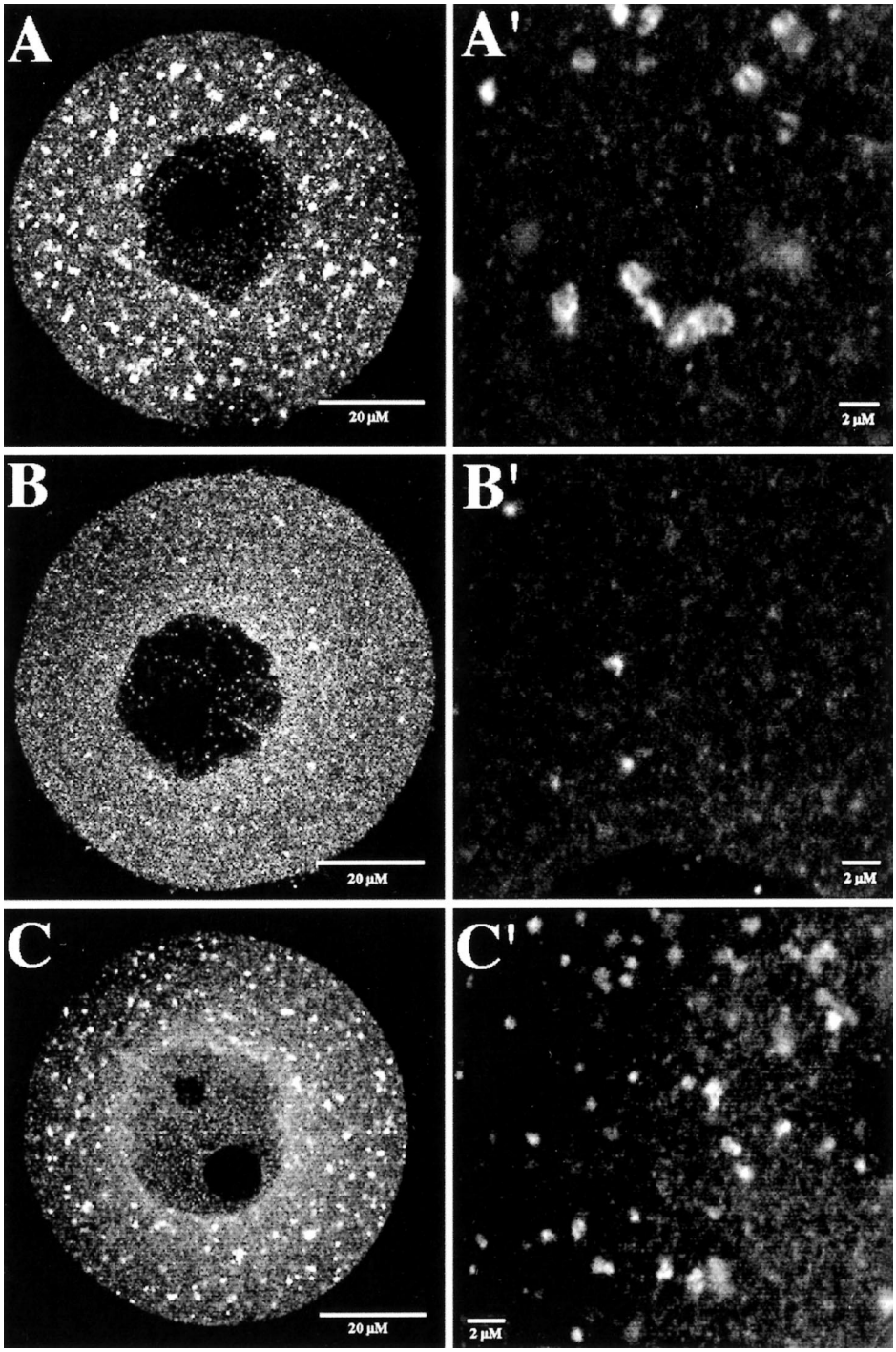

FIG. 5. Confocal imaging of the Golgi apparatus of mouse GV oocytes as affected by brefeldin A. The Golgi apparatus was imaged by immunocytochemistry and confocal microscopy using an antibody directed against the trans-Golgi network protein TGN38. **A**, **A′**) Control. **B**, **B′**) Following a 1-h incubation in M2 medium containing both dbcAMP and 5 μM brefeldin A. **C**, **C′**) Following a 1- to 2-h recovery period in dbcAMP containing M2, after removal of brefeldin A. Equivalent focal planes through the center of the oocyte are shown in each case. **A′**, **B′** and **C′** correspond to higher magnifications of **A**, **B**, and **C**, respectively.

''crown'' surrounding the GV, no defined microtubule organization has been detected in the ooplasm of GV oocytes [43, 44]. This may contribute to the fragmentation of the Golgi apparatus observed in this study. The effect of nocodazole on Golgi apparatus organization is believed to mimic the fragmentation of this organelle during mitosis [26]. Indeed, organelle reorganization is one of the hallmarks of cell division, and during mitosis the cell must guarantee that both daughter cells inherit similar amounts of membrane-bound organelles [23]. In some cases, primarily related to the endoplasmic reticulum and the Golgi apparatus, this involves organelle fragmentation, with concomitant dissemination of vesicular fragments throughout the cytoplasm, before cytokinesis. A more or less homogeneous distribution of these fragments in the cell ensures that each daughter cell will receive approximately half the available material [23]. However, although this stochastic method seems to account for ER inheritance, other authors have suggested that Golgi-derived fragments may interact with the mitotic spindle, and that partitioning of the Golgi apparatus may be more accurate than a random process would predict [45, 46]. There are also conflicting theories regarding what precisely is partitioned during mitosis. Whereas some authors maintain that Golgi and ER partition independently, others suggest that the Golgi collapses into the ER at the onset of mitosis, and reforms from ER exit sites only following telophase [24, 25]. Regardless, many cellular events related to organelle inheritance, including

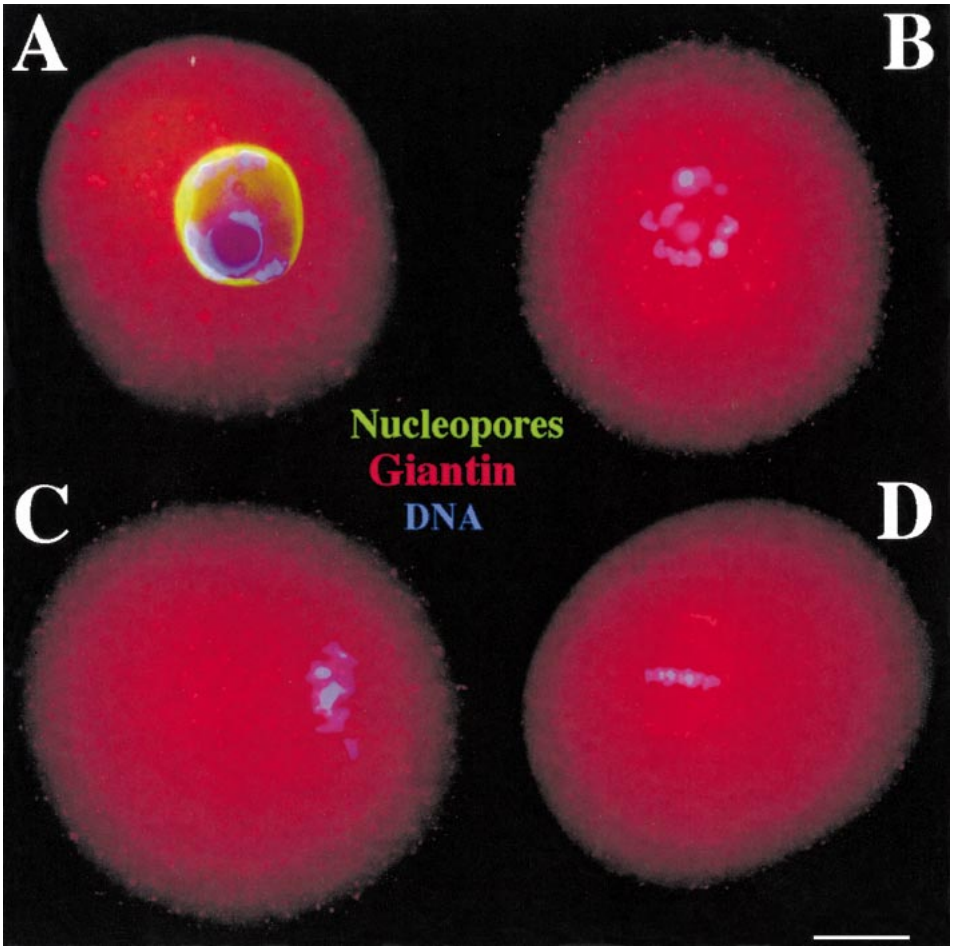

FIG. 6. Golgi apparatus dynamics during mouse oocyte in vitro maturation. The Golgi apparatus of mouse oocytes was labeled by immunocytochemistry using the giantin antibody (red) during several stages of maturation. **A**) GV. **B**) GVBD. **C**) Metaphase I. **D**) Metaphase II. Green, nuclear pore complexes; blue, DNA. Bar = 20 μm.

Golgi fragmentation, also take place during meiosis [16, 21, 22, 47], although asymmetrical division, with concomitant extrusion of polar bodies, limits the loss of precious material from the future female gamete in this case.

Although the Golgi apparatus of somatic cells is fragmented following microtubule depolymerization, it can still export proteins to the plasma membrane, albeit at a lower rate [48]. Similarly, the mini-Golgis in GV oocytes are functionally active, as attested by the energy dependence of the β-COP staining patterns and sensitivity to brefeldin A. In somatic cells this fungal metabolite inhibits protein secretion by inhibiting ER-to-Golgi transport. At the mo-

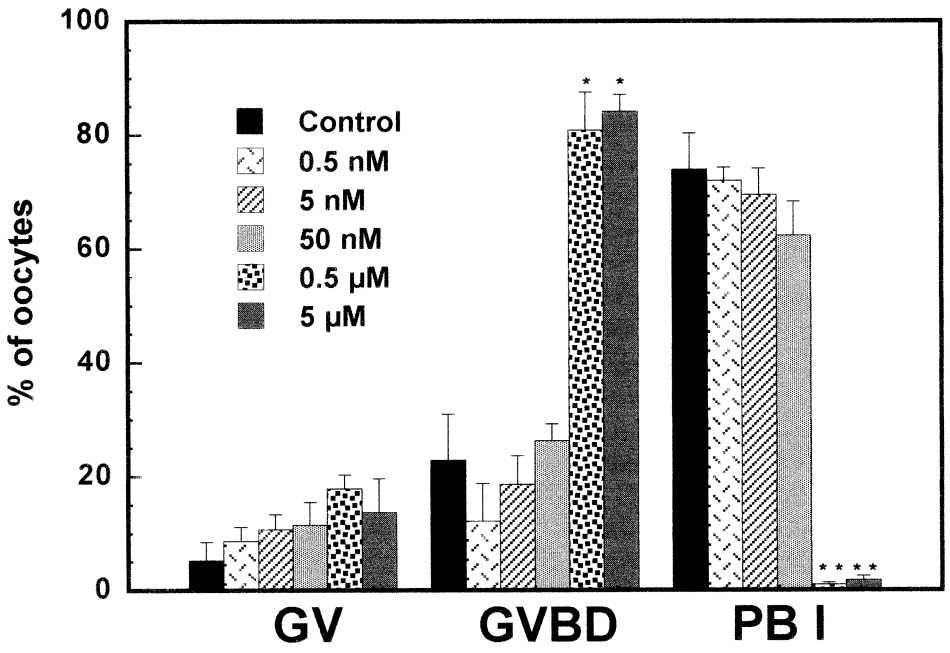

FIG. 7. Effect of brefeldin A on the in vitro maturation of mouse oocytes. Mouse GV oocytes were placed in M2 medium containing varying concentrations of brefeldin A, cultured overnight, and scored the next morning as GV, GVBD, or polar body I oocytes. The graph compiles the data of 5 independent experiments in which a total of 353 oocytes were observed. The average ± SEM is shown in each case. The only significant differences were detected with the two highest concentrations of brefeldin A, in relation to the respective controls. $*P < 0.01$; $**P < 0.001$.

lecular level, brefeldin A acts directly on COPI coat recruitment to membranes [28] via specific ADP-ribosylation factor exchange factors [34, 49]. This results in blocking of vesicle export, but not of Golgi-ER recycling, thus causing the Golgi apparatus to effectively fragment and collapse into the ER. Indeed, we report similar observations in GV oocytes. Incidentally, GTP-γ-S, a nonhydrolyzable GTP analogue, was able to block the effect of brefeldin A on GV oocytes, suggesting the participation of a GTPase in this process, as has been shown in somatic cells [50]. In addition, an inhibitory effect of injected GTP-γ-S on mouse oocyte IVM has been described [51].

Given that brefeldin A acts directly on the formation of COPI-coated vesicles, it could be expected that the distribution of β-COP and giantin, both included in COPI coats [28, 52], is affected by the drug, as was indeed the case. However, the effect of brefeldin A was similar when TGN38, an integral trans-Golgi network-resident protein, was used as a marker. Unlike Golgi stacks, which collapse into the ER in the presence of the drug, the trans-Golgi network forms independent fragments, that accumulate close to the microtubule organizing center following brefeldin A treatment of somatic cells [53, 54]. That all three probes yield similar results (i.e., a diffuse cytoplasmic staining following brefeldin A treatment), leads us to conclude that the drug fragments the different regions of the Golgi apparatus in mouse GV oocytes. Indeed, the concentration of drug needed to disrupt the Golgi was comparable to what has been described for somatic cells [33], and other prominent oocyte structures, such as the cortical granules, seemed unaffected by the treatment. The effect of brefeldin A was fully reversible, and Golgi structures could be reformed if the drug was removed, as has been noted also in somatic cells. Furthermore, recovered oocytes could proceed through IVM when dbcAMP inhibition was lifted.

Large Golgi elements, which are slightly more prevalent in the interior of the oocyte at the GV stage, were replaced with much smaller vesicular structures shortly after the onset of IVM. These vesicles seemed to concentrate at the central part of the oocyte at the GVBD stage, and then spread out into the ooplasm, maintaining a seemingly uniform cytoplasmic distribution throughout IVM, and in metaphase II-arrested oocytes. It has been well established that GV-stage oocytes undergo perinuclear aggregation of organelles during GVBD. These include acidic, lysosome-like organelles [19, 20] and mitochondria [17]; which later disperse in the ooplasm as the first meiotic spindle migrates to the oocyte periphery [20]. That we have made similar observations with Golgi fragments is not unexpected, given that Golgi cisternae have an acidic pH, and can be labeled in vivo with probes directed to lysosomes [55]. These results seem to confirm that ooplasm reorganization at the GVBD stage, including perinuclear aggregation of organelles, is an important feature in meiotic progression, and may play a functional role in maturation [19, 20]. In contrast, the ER has a loose network arrangement in mouse GV oocytes, with few centrally located aggregates, and following IVM it localizes at the cortex, with numerous dense accumulations, possibly related to a reorganization of calcium stores prior to egg activation and cortical granule exocytosis [18, 56].

Regulated secretion is inhibited during mitosis in somatic cells, and newly synthesized proteins are not delivered to the Golgi apparatus and the cell surface [57–59]. Protein secretion is also blocked during maturation in *Xenopus* oocytes [47]. However, in this case the block is downstream from the Golgi apparatus, because ER-to-Golgi and *cis* to medial Golgi transport still take place in mature oocytes [60, 61]. This may constitute a major difference between mitotic and meiotic division. It is interesting to note that although protein secretion is blocked during meiotic maturation, we have shown that brefeldin A is able to reversibly inhibit the IVM of mouse oocytes. It is also interesting that the drug blocks mouse oocyte IVM at the same stage at which it is arrested by protein synthesis inhibitors [2–5]. This effect is likely to be mediated by the brefeldin A-induced disruption of the Golgi apparatus, and ensuing inhibition of membrane trafficking. It is curious that in *Xenopus* oocytes brefeldin A is able to trigger oocyte maturation [62], although the concentration of drug necessary to mimic progesterone-induced maturation was 10 times higher than what is required to affect mammalian somatic and spermatogenic cells [33, 35, 36, 63]. This may reflect some species-specific differences.

Nevertheless, our results suggest that, besides protein synthesis, progression of murine oocyte maturation possibly also requires functional membrane trafficking sometime after GVBD, resulting in either the modification of proteins at the Golgi level, or the delivery of these proteins to appropriate (post-Golgi) sites.

ACKNOWLEDGMENTS

We thank Bryan McVay (ORPRC), Diana Takahashi (ORPRC), and Kimberly Wagle (Pittsburgh Development Center) for technical and editorial assistance. We are also grateful to Dr. Anda Cornea (Confocal Imaging Facility, ORPRC) for helpful suggestions. J.R.-S. wishes to dedicate his portion of this work to the memories of António Paulo Salgado, biologist; Hélder Ribeiro, philosopher; and António Pereira dos Santos, farmer. May we meet again somewhere, my friends.

REFERENCES

1. Schultz RM, Wassarman PM. Specific changes in the pattern of protein synthesis during meiotic maturation of mammalian oocytes in vitro. Proc Natl Acad Sci U S A 1977; 74:538–541.
2. Wassarman PM, Josefowicz WJ, Letourneau GE. Meiotic maturation of mouse oocytes in vitro: inhibition of maturation at specific stages of nuclear progression. J Cell Sci 1976; 22:531–545.
3. Schultz RM, Wassarman PM. Biochemical studies of mammalian oogenesis: protein synthesis during oocyte growth and meiotic maturation in the mouse. J Cell Sci 1977; 24:167–194.
4. Downs SM. Protein synthesis inhibitors prevent both spontaneous and hormone-dependent maturation of isolated mouse oocytes. Mol Reprod Dev 1990; 27:235–243.
5. Motlik J, Rimkevicova Z. Combined effects of protein synthesis and phosphorylation inhibitors on maturation of mouse oocytes in vitro. Mol Reprod Dev 1990; 27:230–234.
6. Ekholm C, Magnusson C. Rat oocyte maturation: effects of protein synthesis inhibitors. Biol Reprod 1979; 21:1287–1293.
7. Fulka J Jr, Motlik J, Fulka J, Jilek F. Effect of cycloheximide on nuclear maturation of pig and mouse oocytes. J Reprod Fertil 1986; 77:281–285.
8. Hunter AG, Moor RM. Stage-dependent effects of inhibiting ribonucleic acids and protein synthesis on meiotic maturation of bovine oocytes in vitro. J Dairy Sci 1987; 70:1646–1651.
9. Moor RM, Crosby IM. Protein requirements for germinal vesicle breakdown in ovine oocytes. J Embryol Exp Morphol 1986; 94:207–220.
10. Ledan E, Polanski Z, Terret ME, Maro B. Meiotic maturation of the mouse oocyte requires an equilibrium between cyclin B synthesis and degradation. Dev Biol 2001; 232:400–413.
11. Polanski Z, Ledan E, Brunet S, Louvet S, Verlhac MH, Kubiak JZ, Maro B. Cyclin synthesis controls the progression of meiotic maturation in mouse oocytes. Development 1998; 125:4989–4997.
12. Hampl A, Eppig JJ. Analysis of the mechanism(s) of metaphase I arrest in maturing mouse oocytes. Development 1995; 121:925–933.
13. Hashimoto N, Kishimoto T. Regulation of meiotic metaphase by a

cytoplasmic maturation-promoting factor during mouse oocyte maturation. Dev Biol 1988; 126:242–252.
14. Clarke HJ, Masui Y. The induction of reversible and irreversible chromosome decondensation by protein synthesis inhibition during meiotic maturation of mouse oocytes. Dev Biol 1983; 97:291–301.
15. Wassarman PM, Josefowicz WJ. Oocyte development in the mouse: an ultrastructural comparison of oocytes isolated at various stages of growth and competence. J Morphol 1978; 156:209–235.
16. Weakley BS, Webb P, James JL. Cytochemistry of the Golgi apparatus in developing ovarian germ cells of the Syrian hamster. Cell Tissue Res 1981; 220:349–372.
17. Van Blerkom J, Runner MN. Mitochondrial reorganization during resumption of arrested meiosis in the mouse oocyte. Am J Anat 1984; 171:335–355.
18. Mehlmann LM, Terasaki M, Jaffe LA, Kline D. Reorganization of the endoplasmic reticulum during meiotic maturation of the mouse oocyte. Dev Biol 1995; 170:607–615.
19. Ezzell RM, Szego CM. Luteinizing hormone-accelerated redistribution of lysosome-like organelles preceding dissolution of the nuclear envelope in rat oocytes maturing in vitro. J Cell Biol 1979; 82:264–277.
20. Albertini DF. Cytoplasmic reorganization during the resumption of meiosis in cultured preovulatory rat oocytes. Dev Biol 1987; 120:121–131.
21. Calarco PG, Donahue RP, Szollosi D. Germinal vesicle breakdown in the mouse oocyte. J Cell Sci 1972; 10:369–385.
22. Weakley BS. Electron microscopy of the oocyte and granulosa cells in the developing ovarian follicles of the golden hamster (*Mesocricetus auratus*). J Anat 1966; 100:503–534.
23. Warren G, Wickner W. Organelle inheritance. Cell 1996; 84:395–400.
24. Roth MG. Inheriting the Golgi. Cell 1999; 99:559–562.
25. Nelson WJ. W(h)ither the Golgi during mitosis? J Cell Biol 2000; 149:243–348.
26. Thyberg J, Moskalewski S. Role of microtubules in the organization of the Golgi complex. Exp Cell Res 1999; 246:263–279.
27. Rothman JE. Mechanisms of intracellular protein transport. Nature 1994; 372:55–63.
28. Lowe M, Kreis TE. Regulation of membrane traffic in animal cells by COPI. Biochim Biophys Acta 1998; 1404:53–66.
29. Pfeffer SR. Transport-vesicle targeting: tethers before SNAREs. Nat Cell Biol 1999; 1:E17–E22.
30. Nichols BJ, Pelham HR. SNAREs and membrane fusion in the Golgi apparatus. Biochim Biophys Acta 1998; 1404:9–31.
31. Glick BS, Malhotra V. The curious status of the Golgi apparatus. Cell 1998; 95:883–889.
32. Allan BB, Balch WE. Protein sorting by directed maturation of Golgi compartments. Science 1999; 285:63–66.
33. Lippincott-Schwartz J, Yuan LC, Bonifacino JS, Klausner RD. Rapid redistribution of Golgi proteins into the ER in cells treated with brefeldin A: evidence for membrane cycling from Golgi to ER. Cell 1989; 56:801–813.
34. Peyroche A, Paris S, Jackson CL. Nucleotide exchange on ARF mediated by yeast Gea1 protein. Nature 1996; 384:479–481.
35. Moreno RD, Ramalho-Santos J, Sutovsky P, Chan EKL, Schatten G. Vesicular traffic and Golgi apparatus dynamics during mammalian spermatogenesis: implications for acrosome architecture. Biol Reprod 2000; 63:89–98.
36. Ramalho-Santos J, Moreno RD, Wessel GM, Chan EK, Schatten G. Membrane trafficking machinery components associated with the mammalian acrosome during spermiogenesis. Exp Cell Res 2001; 267:45–60.
37. Sutovsky P, Simerly C, Hewitson L, Schatten G. Assembly of nuclear pore complexes and annulate lamellae promotes normal pronuclear development in fertilized mammalian oocytes. J Cell Sci 1998; 111: 2841–2854.
38. Fulton BP, Whittingham DG. Activation of mammalian oocytes by intracellular injection of calcium. Nature 1978; 273:149–151.
39. Tombes RM, Simerly C, Borisy GG, Schatten G. Meiosis, egg activation, and nuclear envelope breakdown are differentially reliant on Ca2+, whereas germinal vesicle breakdown is Ca2+ independent in the mouse oocyte. J Cell Biol 1992; 117:799–811.
40. Ramalho-Santos J, Sutovsky P, Simerly C, Oko R, Wessel GM, Hewitson L, Schatten G. ICSI choreography: fate of sperm structures after monospermic rhesus ICSI and first cell cycle implications. Hum Reprod 2000; 15:2610–2620.
41. Pagano RE, Martin OC, Kang HC, Haugland RP. A novel fluorescent ceramide analogue for studying membrane traffic in animal cells: accumulation at the Golgi apparatus results in altered spectral properties of the sphingolipid precursor. J Cell Biol 1991; 113:1267–1279.
42. Ducibella T, Anderson E, Albertini DF, Aalberg J, Rangarajan S. Quantitative studies of changes in cortical granule number and distribution in the mouse oocyte during meiotic maturation. Dev Biol 1988; 130:184–197.
43. Rime H, Jessus C, Ozon R. Distribution of microtubules during the first meiotic cell division in the mouse oocyte: effect of taxol. Gamete Res 1987; 17:1–13.
44. Alexandre H, Van Cauwenberge A, Mulnard J. Involvement of microtubules and microfilaments in the control of the nuclear movement during maturation of mouse oocyte. Dev Biol 1989; 136:311–320.
45. Shima DT, Cabrera-Poch N, Pepperkok R, Warren G. An ordered inheritance strategy for the Golgi apparatus: visualization of mitotic disassembly reveals a role for the mitotic spindle. J Cell Biol 1998; 141: 955–966.
46. Shima DT, Haldar K, Pepperkok R, Watson R, Warren G. Partitioning of the Golgi apparatus during mitosis in living HeLa cells. J Cell Biol 1997; 137:1211–1228.
47. Colman A, Jones EA, Heasman J. Meiotic maturation in *Xenopus* oocytes: a link between the cessation of protein secretion and the polarized disappearance of Golgi apparati. J Cell Biol 1985; 101:313–318.
48. Rogalski AA, Bergmann JE, Singer SJ. Effect of microtubule assembly status on the intracellular processing and surface expression of an integral protein of the plasma membrane. J Cell Biol 1984; 99:1101–1109.
49. Peyroche A, Antonny B, Robineau S, Acker J, Cherfils J, Jackson CL. Brefeldin A acts to stabilize an abortive ARF-GDP-Sec7 domain protein complex: involvement of specific residues of the Sec7 domain. Mol Cell 1999; 3:275–285.
50. Scheel J, Pepperkok R, Lowe M, Griffiths G, Kreis TE. Dissociation of coatomer from membranes is required for brefeldin A-induced transfer of Golgi enzymes to the endoplasmic reticulum. J Cell Biol 1997; 137:319–333.
51. Downs SM, Buccione R, Eppig JJ. Modulation of meiotic arrest in mouse oocytes by guanyl nucleotides and modifiers of G-proteins. J Exp Zool 1992; 262:391–404.
52. Chan EKL, Fritzler MJ. Golgins: Coiled-coil-rich proteins associated with the Golgi complex. Elec J Biotech 1998; 1:1–10.
53. Ladinsky MS, Howell KE. The trans-Golgi network can be dissected structurally and functionally from the cisternae of the Golgi complex by brefeldin A. Eur J Cell Biol 1992; 59:92–105.
54. Reaves B, Banting G. Perturbation of the morphology of the trans-Golgi network following Brefeldin A treatment: redistribution of a TGN-specific integral membrane protein, TGN38. J Cell Biol 1992; 116:85–94.
55. Moreno RD, Ramalho-Santos J, Wessel GM, Chan EKL, Schatten G. The Golgi apparatus segregates from the lysosomal/acrosomal vesicle during rhesus spermiogenesis: structural alterations. Dev Biol 2000; 219:334–349.
56. Ducibella T, Rangarajan S, Anderson E. The development of mouse oocyte cortical reaction competence is accompanied by major changes in cortical vesicles and not cortical granule depth. Dev Biol 1988; 130:789–792.
57. Warren G, Featherstone C, Griffiths G, Burke B. Newly synthesized G protein of vesicular stomatitis virus is not transported to the cell surface during mitosis. J Cell Biol 1983; 97:1623–1628.
58. Hesketh TR, Beaven MA, Rogers J, Burke B, Warren GB. Stimulated release of histamine by a rat mast cell line is inhibited during mitosis. J Cell Biol 1984; 98:2250–2254.
59. Featherstone C, Griffiths G, Warren G. Newly synthesized G protein of vesicular stomatitis virus is not transported to the Golgi complex in mitotic cells. J Cell Biol 1985; 101:2036–2046.
60. Ceriotti A, Colman A. Protein transport from endoplasmic reticulum to the Golgi complex can occur during meiotic metaphase in *Xenopus* oocytes. J Cell Biol 1989; 109:1439–4144.
61. Leaf DS, Roberts SJ, Gerhart JC, Moore HP. The secretory pathway is blocked between the trans-Golgi and the plasma membrane during meiotic maturation in *Xenopus* oocytes. Dev Biol 1990; 141:1–12.
62. Mulner-Lorillon O, Belle R, Cormier P, Drewing S, Minella O, Poulhe R, Schmalzing G. Brefeldin A provokes indirect activation of cdc2 kinase (MPF) in *Xenopus* oocytes, resulting in meiotic cell division. Dev Biol 1995; 170:223–229.
63. West AP, Willison KR. Brefeldin A and mannose 6-phosphate regulation of acrosomic related vesicular trafficking. Eur J Cell Biol 1996; 70:315–321.